

## Quantized nonadiabatic coupling terms of $\text{H}_3^+$

Alexander Alijah,\* Julien Fremont, and Vladimir G. Tyuterev

*Groupe de Spectrométrie Moléculaire et Atmosphérique (GSMA), UMR CNRS 7331, Université de Reims Champagne-Ardenne, Campus Moulin de la Housse, Boîte Postale 1039, 51687 Reims Cedex 2, France*

(Received 6 May 2015; published 16 July 2015)

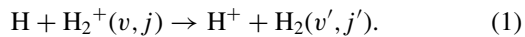
Nonadiabatic coupling terms between the four lowest singlet states of  $\text{H}_3^+$  were calculated *ab initio*. The analysis according to the criteria suggested by Baer and Alijah [Baer and Alijah, *Chem. Phys. Lett.* **319**, 489 (2000)] shows that as many as four electronic states may be required for an accurate description of the reactions  $\text{H} + \text{H}_2^+(v, j) \rightleftharpoons \text{H}^+ + \text{H}_2(v', j')$ , depending on the collision energy.

DOI: [10.1103/PhysRevA.92.012704](https://doi.org/10.1103/PhysRevA.92.012704)

PACS number(s): 34.70.+e, 31.10.+z, 31.15.X-, 31.30.-i

### I. INTRODUCTION

When the simplest atom, H, hits the simplest molecule,  $\text{H}_2^+$ , there are four possible outcomes: elastic or inelastic scattering, breakup of the  $\text{H}_2^+$  molecule, or the formation of  $\text{H}_2$ ,

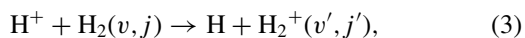


Here,  $v$  and  $j$  denote the vibrational and rotational quantum numbers, respectively. The latter process proceeds either via charge transfer or via proton exchange, as investigated by Last *et al.* [1]. The reaction is of great importance for the chemistry in diffuse clouds [2] where the fraction of molecular hydrogen is relatively small so that the hydrogen atom becomes an important reaction partner for  $\text{H}_2^+$ . Reaction (1) looks simple; however, it is not. Let us assume that the collision partners are in their electronic ground states. The lowest electronic state,  $\tilde{X}^1A'$ , of the underlying triatomic,  $\text{H}_3^+$ , dissociates to  $\text{H}^+ + \text{H}_2(\tilde{X}^1\Sigma_g^+)$ ; hence, the entrance channel is located on an excited electronic state surface. In other words, reaction (1) is a nonadiabatic reaction.

There are three avoided crossings between the two lowest singlet states of  $\text{H}_3^+$ ,  $\tilde{X}^1A'$  and  $\tilde{B}^1\Sigma^+$ , one in each diatomic channel. These avoided crossings occur at the internuclear H-H distance of  $r_{ac} = 2.5017a_0$ , since for this distance the energies of  $\text{H}_2 + \text{H}^+$  and  $\text{H}_2^+ + \text{H}$  coincide; i.e.,

$$V(\text{H}_2, r = r_{ac}) = V(\text{H}_2^+, r = r_{ac}) - \frac{1}{2}. \quad (2)$$

For  $r = r_{ac}$ , the energy gap between the two electronic states diminishes with increasing  $R$ , the scattering coordinate, and approaches zero as  $R$  goes to infinity. In addition to these avoided crossing seams, there is a conical intersection line at equilateral configurations between the first and second excited singlet states demanded by symmetry. Even though the minimum of the intersection line is at very high energy and the depth of the third state is only  $20 \text{ cm}^{-1}$  [3], the third state might affect reaction (1) or its reverse,



due to the topological effect on the wave function, i.e., the building up of a geometrical or Berry phase [4].

Reaction (3) is endothermic and possible if the collision energy is sufficiently high, about four vibrational quanta

of  $\text{H}_2$ . It was investigated by a three-dimensional quantum scattering approach in a seminal contribution by Baer *et al.* [5] which describes well the experimental data obtained by Niedner *et al.* [6] at laboratory energy  $E_{\text{lab}} = 30 \text{ eV}$ . In their article, potential energy surfaces of the two lowest states were obtained, as well as nonadiabatic coupling terms, using the diatomics in molecules (DIM) [7] representation. The infinite-order sudden approximation was used to describe nonadiabatic transitions. In a recent joint experimental and theoretical work [8] the low-energy region was studied and a long-standing discrepancy resolved. A review on the dynamics and importance of this reaction was published by Gonzalez-Lezana and Honvault [9].

Many more studies have been performed in recent years (see, for example, Refs. [10,11] and references therein), all on two coupled potential energy surfaces. The overall success of all these theoretical investigations appears to indicate that the charge transfer processes in reactions (1) and (3) proceed by and large on two surfaces, at least for the collision energies considered in those papers.

Barragán [12], investigating these two reactions and also providing an excellent overview of the literature, raised a question of interest for the present study: Are two potential energy surfaces sufficient? The conclusion was that three or more electronic states should be considered simultaneously. This work was followed by a three-state semiclassical trajectory study [13] which was, however, not really conclusive.

In the present study we offer evidence that four electronic surfaces are necessary for a complete description. Our investigation is based on the *ab initio* calculation of nonadiabatic coupling terms (NACTs) between the four lowest singlet states and their analysis in terms of the quantization condition suggested by Baer and Alijah [14]. During the final preparation of this paper we became aware of a recent study by Adhikari and co-workers [15], who applied the same method to the title system and computed NACTs for the three lowest singlet states. The present contribution extends this to the four lowest singlet states.

### II. THEORY

The investigation of the nuclear motion in molecules is very often performed within the adiabatic approach aiming at a separation of nuclear and electronic motions. Since the separation is not exact, nuclear-electronic kinetic coupling terms arise that may cause nonadiabatic transitions [16] of

\*alexander.aliyah@univ-reims.fr

nuclei evolving initially on one single surface. The adiabatic equations can be written as

$$\mathbf{I} \frac{\nabla^2}{2m} \xi + \frac{1}{m} \boldsymbol{\tau}^{(1)} \nabla \xi + \left( \frac{1}{2m} \boldsymbol{\tau}^{(2)} + \mathbf{V} - \mathbf{I} E \right) \xi = 0, \quad (4)$$

where summation over all nuclei is implied.  $\mathbf{I}$  denotes the identity matrix,  $\xi^\dagger = [\xi_1(R), \xi_2(R), \dots, \xi_N(R)]$  the nuclear wave functions corresponding to the electronic wave functions  $\Phi_1, \Phi_2, \dots, \Phi_N$ , and

$$\tau_{ij}^{(1)} = \langle \Phi_i | \nabla \Phi_j \rangle, \quad (5)$$

$$\tau_{ij}^{(2)} = \langle \Phi_i | \nabla^2 \Phi_j \rangle, \quad (6)$$

$$V_{ij} = V_i(R) \delta_{ij}. \quad (7)$$

The matrix elements of  $\boldsymbol{\tau}^{(1)}$  are coupling vectors (gradients). For a particular nuclear coordinate  $R_s$ , the corresponding nonadiabatic coupling term is

$$\tau_{ij;R_s}^{(1)} = \left\langle \Phi_i \left| \frac{\partial \Phi_j}{\partial R_s} \right. \right\rangle. \quad (8)$$

Such coupling terms become large if the electronic states  $i$  and  $j$  are close in energy and will be infinite at points of degeneracy. In these cases, the adiabatic approximation, in which only one electronic state is retained, breaks down, making a two-state adiabatic treatment necessary. In view of the singular behavior of the NACTs one may seek a transformation that minimizes their size and, in the ideal case of the so-called strictly diabatic representation, removes them completely. This requires the existence of a solution,  $\mathbf{A}$ , to the differential equation

$$\nabla \mathbf{A} + \boldsymbol{\tau}^{(1)} \mathbf{A} = 0. \quad (9)$$

Baer [17] showed that, in order for such a solution  $\mathbf{A}$  to exist, the coupling vectors  $\boldsymbol{\tau} \equiv \tau_{ij}^{(1)}$  must satisfy the ‘‘curl condition’’

$$\text{curl } \boldsymbol{\tau} \equiv \nabla \times \boldsymbol{\tau} = \boldsymbol{\tau} \times \boldsymbol{\tau}. \quad (10)$$

A unitary transformation of the Hamiltonian with the matrix  $\mathbf{A}$  removes the kinetic coupling terms but introduces equivalent coupling terms into the potential matrix,

$$\mathbf{W} = \mathbf{A}^\dagger \mathbf{V} \mathbf{A}, \quad (11)$$

where  $\mathbf{V}$  and  $\mathbf{W}$  are the adiabatic and diabatic potential matrices, respectively. In the general case, a unique solution of Eq. (9) cannot be found and therefore a ‘‘strictly’’ diabatic representation does not exist [18]. One particular part of the derivative coupling can, however, be removed, namely the longitudinal part along a certain path. If such a path is chosen wisely, meaningful diabatic potentials are obtained. Let us consider a closed path along a circular coordinate  $\varphi$  such that

$$\mathbf{V}(\varphi, R_i) = \mathbf{V}(\varphi + 2\pi, R_i), \quad (12)$$

where  $R_i$  denote the remaining internal coordinates. A diabatic potential matrix should be single valued and thus satisfy just as the adiabatic potential the condition

$$\mathbf{W}(\varphi, R_i) = \mathbf{W}(\varphi + 2\pi, R_i). \quad (13)$$

For simplicity and without loss of generality, let us consider the case of two coupled electronic states. Since the adiabatic-

diabatic transformation matrix can be expressed as

$$\begin{aligned} \mathbf{A}(\varphi) &= \begin{pmatrix} \cos \theta_{12}(\varphi) & \sin \theta_{12}(\varphi) \\ -\sin \theta_{12}(\varphi) & \cos \theta_{12}(\varphi) \end{pmatrix} \\ &= \begin{pmatrix} \cos \int_0^\varphi \tau_{12;\varphi} d\varphi' & \sin \int_0^\varphi \tau_{12;\varphi} d\varphi' \\ -\sin \int_0^\varphi \tau_{12;\varphi} d\varphi' & \cos \int_0^\varphi \tau_{12;\varphi} d\varphi' \end{pmatrix}, \end{aligned} \quad (14)$$

a meaningful diabatic potential exists only if the coupling terms  $\tau_{ij;\varphi}$  satisfy the quantization condition [14]

$$\begin{aligned} \theta_{12}(2\pi) - \theta_{12}(0) &= \int_0^{2\pi} \tau_{12;\varphi} d\varphi = n\pi, \\ n &= 0, \pm 1, \pm 2, \dots \end{aligned} \quad (15)$$

In the three-state case  $\mathbf{A}$  depends on three angles and can be expanded as a product of three rotation matrices, e.g.,

$$\mathbf{A}(\theta_{12}, \theta_{23}, \theta_{13}) = \mathbf{A}^{(12)}(\theta_{12}) \mathbf{A}^{(23)}(\theta_{23}) \mathbf{A}^{(13)}(\theta_{13}). \quad (16)$$

The order of the three matrices on the right-hand side is arbitrary and, hence, six equivalent representations of the  $\mathbf{A}$  matrix exist which belong to two groups:  $(12) \times (23) \times (13)$  and cyclic permutations, and  $(12) \times (13) \times (23)$  and cyclic permutations. Inserting  $\mathbf{A}$  into Eq. (9), a system of coupled equations is obtained for the transformation angles [19]. For the first group of matrices  $\mathbf{A}$ , this system becomes

$$\begin{aligned} \nabla \theta_{ij} &= -\tau_{ij} - \tan \theta_{jk} (\tau_{jk} \sin \theta_{ij} - \tau_{ik} \cos \theta_{ij}), \\ \nabla \theta_{jk} &= -(\tau_{ik} \sin \theta_{ij} + \tau_{jk} \cos \theta_{ij}), \\ \nabla \theta_{ik} &= -(-1)^p (\cos \theta_{jk})^{-1} (\tau_{jk} \sin \theta_{ij} - \tau_{ik} \cos \theta_{ij}), \end{aligned} \quad (17)$$

where  $p = 0$  for the first and third products of transformation matrices, and  $p = 1$  for the second product. These systems may be integrated subject to the initial condition  $\theta_{lm} = 0$ . The quantization condition Eq. (13) is then satisfied if  $\theta_{lm}(2\pi) = n\pi$ , with  $n = 0, \pm 1, \pm 2, \dots$ . Since the first application of this procedure by Baer and co-workers [20,21], it has been widely used for the diabatization of potential energy surfaces (see Ref. [22] and references therein).

### III. THE $\text{H}_3^+$ SYSTEM

$\text{H}_3^+$  is a stable molecule and possesses around 80 000 bound or quasibound vibrational rotational states [23]. Recently a very accurate potential energy surface for the ground state,  $X^1A'$ , was obtained by Pavanello and co-workers [24]. It is based on *ab initio* electronic energy points computed with correlated shifted Gaussians [25] and contains diagonal adiabatic and relativistic corrections. The quality of this surface permitted the study of nonadiabatic [26] and QED [27] effects on the vibrational states. Highly accurate calculations have also been reported by Jaquet and Carrington [28]. For the two lowest excited singlet states of  $\text{H}_3^+$  potential energy surfaces were obtained by Viegas *at al.* [3] and recently by Adhikari *at al.* [15], both using standard *ab initio* methods. Figure 1 offers a view of the four lowest singlet states. Table I contains a summary of characteristic energies of singlet  $\text{H}_3^+$ , taken from Ref. [3].

To answer the question as to how many electronic states are needed for an accurate description of the title reaction,

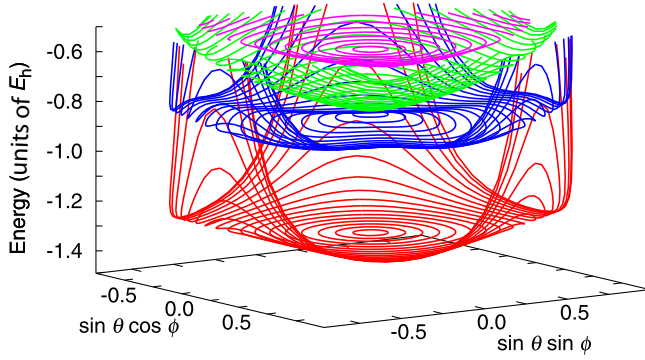


FIG. 1. (Color online) Potential energy surfaces of the four lowest singlet states of  $H_3^+$  in a hyperspherical representation with the hyper-radius fixed at  $\rho = 3.0a_0$ . The equilateral configuration is at the center of the figure. This configuration corresponds to the minimum of the ground-state surface, while a conical intersection occurs between the first and second excited states.

we suggest the following two-step procedure: First, a suitable coordinate system is chosen, in which a closed path can be defined such that the major coupling terms are eliminated. Second, the fulfillment of the quantization condition of the NACTs for various nuclear configurations and as a function of the number of electronic states is tested. If the quantization condition is fulfilled and thus Eq. (13), the electronic states included are sufficient as they form a Hilbert subspace. The charge transfer process  $H_2^+ + H \rightarrow H_2 + H^+$  is nonadiabatic and involves at least the electronic ground state of  $H_3^+$  and the first excited singlet state [5]. Three avoided crossings occur if two atoms are separated by  $r_{ac} = 2.5017a_0$  and the third atom is at a large distance. There is also a conical intersection between the first and second excited states at equilateral triangular configurations. The coupling vector  $\tau_{23}$  has thus a singular polar component along the  $D_{3h}$  intersection line. Can we transform this singular component away? A suitable coordinate system can be found readily; it is that of democratic hyperspherical coordinates, which we use in the definition of Johnson [29]. The three internal hyperspherical coordinates are  $\rho$ , the hyper-radius, and  $\theta_{hyp}$  and  $\phi$ , the hyperangles. The three external coordinates are the Euler angles  $\alpha$ ,  $\beta$ , and  $\gamma$ . The symbol  $\Omega$  is used to denote the five angles. In the hyperspherical coordinate system, the conical intersection at  $D_{3h}$  configurations is mapped to the north pole,  $\theta_{hyp} = 0$ , with  $\rho$  following (for  $\theta_{hyp} = 0$ ) the intersection line. The angle  $\phi$  is not defined at the pole, but for small displacement,  $\theta_{hyp} \neq 0$ , encircles the conical intersection.  $\phi$  is thus a natural

TABLE I. Characteristic energy values for singlet  $H_3^+$ .

Threshold	$E/\text{cm}^{-1}$
$2H + H^+$	38 292.84
$V_{\min}(H_3^+, 3^1E)$	38 271.55
$V(H_2, r = r_{ac})$	17 675.83
$H_2^+ + H$ isomerization barrier	38 060.32
$H_2^+ + H$ dissociation energy	15 767.27
$V_{\min}(H_3^+, B^1\Sigma^+)$	15 710.20
$H_2 + H^+$ dissociation energy	0.0
$V_{\min}(H_3^+, X^1A_1')$	-37 169.71

representative of the generic cyclic variable  $\phi$  introduced in Eq. (12). In the hyperspherical coordinates, the matrix elements between electronic states  $|\Phi_i\rangle$  and  $|\Phi_j\rangle$  of the nuclear Hamiltonian read

$$\begin{aligned}
 H_{ij}^n(\rho, \Omega) = & -\frac{1}{2\mu} \left\{ \frac{\partial^2}{\partial \rho^2} - \frac{\Lambda^2(\Omega) + \frac{15}{4}}{\rho^2} \right\} \delta_{ij} \\
 & - \frac{1}{2\mu} \left\{ \left\langle \Phi_i \left| \frac{\partial^2 \Phi_j}{\partial \rho^2} \right. \right\rangle - \frac{\langle \Phi_i | \Lambda^2 | \Phi_j \rangle}{\rho^2} \right\} \\
 & - \frac{1}{2\mu} \left\{ 2 \left\langle \Phi_i \left| \frac{\partial \Phi_j}{\partial \rho} \right. \right\rangle \frac{\partial}{\partial \rho} + \frac{8 \sin^2 \theta_{hyp}}{\rho^2} \right. \\
 & \times \left. \left\langle \Phi_i \left| \frac{\partial \Phi_j}{\partial \cos \theta_{hyp}} \right. \right\rangle \frac{\partial}{\partial \cos \theta_{hyp}} \right. \\
 & \left. + \frac{8}{\rho^2 \sin^2 \theta_{hyp}} \left\langle \Phi_i \left| \frac{\partial \Phi_j}{\partial \phi} \right. \right\rangle \frac{\partial}{\partial \phi} \right\}, \quad (18)
 \end{aligned}$$

where  $\mu = \sqrt{m_1 m_2 m_3 / (m_1 + m_2 + m_3)}$  is the three-particle reduced mass and  $\Lambda^2(\Omega)$  the grand angular momentum operator [30]. As the  $\frac{\partial^2}{\partial \phi^2}$  coupling term contains the factor  $\rho^{-2} \sin^{-2} \theta_{hyp}$ , which becomes singular at the pole, we seek a transformation to remove it. There is a particularity with respect to these hyperspherical coordinates: the internal angle  $\phi$  and the Euler angle  $\gamma$  are connected through the mixed coupling term  $\frac{\partial^2}{\partial \phi \partial \gamma}$  inside the  $\Lambda^2(\Omega)$  operator, and the cyclic boundary condition for the wave function becomes

$$\Psi(\rho, \theta_{hyp}, \phi, \alpha, \beta, \gamma) = \Psi(\rho, \theta_{hyp}, \phi + 2\pi, \alpha, \beta, \gamma + \pi). \quad (19)$$

To eliminate the rotation induced by the  $\gamma$  angle, we set  $\gamma = \phi/2$ .

For our computations of the NACTs, Cartesian coordinates of the three particles,  $i = 1, 2, 3$ , were required. They were obtained with help of the general transformation formula

$$\begin{aligned}
 x_i = & X + \frac{\sqrt{2}\sqrt{3}}{3} \rho \cos(\alpha) \cos(\beta) \cos(\gamma) \sin\left(\frac{\pi}{4} + \frac{\theta_{hyp}}{2}\right) \cos\left(\frac{\pi}{4} + \frac{\phi}{2} + \frac{2i\pi}{3}\right) + \frac{\sqrt{2}\sqrt{3}}{3} \rho \sin(\alpha) \cos(\beta) \sin(\gamma) \\
 & \times \cos\left(\frac{\pi}{4} + \frac{\theta_{hyp}}{2}\right) \sin\left(\frac{\pi}{4} + \frac{\phi}{2} + \frac{2i\pi}{3}\right) - \frac{\sqrt{2}\sqrt{3}}{3} \rho \sin(\alpha) \sin(\gamma) \sin\left(\frac{\pi}{4} + \frac{\theta_{hyp}}{2}\right) \cos\left(\frac{\pi}{4} + \frac{\phi}{2} + \frac{2i\pi}{3}\right) \\
 & + \frac{\sqrt{2}\sqrt{3}}{3} \rho \cos(\alpha) \sin(\gamma) \cos\left(\frac{\pi}{4} + \frac{\theta_{hyp}}{2}\right) \sin\left(\frac{\pi}{4} + \frac{\phi}{2} + \frac{2i\pi}{3}\right),
 \end{aligned}$$

$$\begin{aligned}
y_i &= Y - \frac{\sqrt{2}\sqrt[4]{3}}{3}\rho \cos(\alpha) \cos(\beta) \sin(\gamma) \sin\left(\frac{\pi}{4} + \frac{\theta_{\text{hyp}}}{2}\right) \cos\left(\frac{\pi}{4} + \frac{\phi}{2} + \frac{2i\pi}{3}\right) - \frac{\sqrt{2}\sqrt[4]{3}}{3}\rho \sin(\alpha) \cos(\beta) \sin(\gamma) \\
&\quad \times \cos\left(\frac{\pi}{4} + \frac{\theta_{\text{hyp}}}{2}\right) \sin\left(\frac{\pi}{4} + \frac{\phi}{2} + \frac{2i\pi}{3}\right) - \frac{\sqrt{2}\sqrt[4]{3}}{3}\rho \sin(\alpha) \sin(\gamma) \sin\left(\frac{\pi}{4} + \frac{\theta_{\text{hyp}}}{2}\right) \cos\left(\frac{\pi}{4} + \frac{\phi}{2} + \frac{2i\pi}{3}\right) \\
&\quad + \frac{\sqrt{2}\sqrt[4]{3}}{3}\rho \cos(\alpha) \cos(\gamma) \cos\left(\frac{\pi}{4} + \frac{\theta_{\text{hyp}}}{2}\right) \sin\left(\frac{\pi}{4} + \frac{\phi}{2} + \frac{2i\pi}{3}\right), \\
z_i &= Z - \frac{\sqrt{2}\sqrt[4]{3}}{3}\rho \cos(\alpha) \sin(\beta) \sin\left(\frac{\pi}{4} + \frac{\theta_{\text{hyp}}}{2}\right) \cos\left(\frac{\pi}{4} + \frac{\phi}{2} + \frac{2i\pi}{3}\right) - \frac{\sqrt{2}\sqrt[4]{3}}{3}\rho \sin(\alpha) \sin(\beta) \\
&\quad \times \cos\left(\frac{\pi}{4} + \frac{\theta_{\text{hyp}}}{2}\right) \sin\left(\frac{\pi}{4} + \frac{\phi}{2} + \frac{2i\pi}{3}\right),
\end{aligned} \tag{20}$$

where  $X$ ,  $Y$ , and  $Z$  denote the Cartesian coordinates of the center of mass. The above expressions may be simplified by fixing the two remaining Euler angles  $\alpha$  and  $\beta$  at the convenient values  $\alpha = 0$  and  $\beta = 0$ . Equally, the center-of-mass coordinates were set to zero. Since these coordinates are not related to the internal motion of the molecule, their values are arbitrary for the purpose of the present study. In our computations, we used a grid of coordinates defined by  $30^\circ \leq \phi \leq 90^\circ$ ,  $\Delta\phi = 5^\circ$  and  $0^\circ \leq \theta_{\text{hyp}} \leq 90^\circ$ ,  $\Delta\theta_{\text{hyp}} = 5^\circ$ . The hyper-radius was kept at a representative value,  $\rho = 3.0a_0$ , which corresponds roughly to the value at the minimum of the electronic ground state. Cartesian coordinates were then generated with help of the transformation formulas (20) to obtain input data for the *ab initio* calculations. The MOLPRO [31] package was employed at the CISD/cc-pV5Z level of theory. NACTs were generated by the three-point finite differences procedure DDR with  $\Delta\phi = 0.1^\circ$ .

#### IV. RESULTS AND DISCUSSION

Before integrating the coupled equations (17), the computed NACTs need to be inspected carefully and corrected if the phase of one of the electronic wave functions has changed within our set of calculations. We keep the phases of the  $\theta_{\text{hyp}} = 5^\circ$  functions. The behavior of the NACTs connecting the four lowest singlet states are shown in Fig. 2. At  $\theta_{\text{hyp}} = 0^\circ$ , the north pole, the angle of longitude,  $\phi$ , is not defined. All coupling terms are zero, except for  $\tau_{23}$ , which is one-half due to the conical intersection between states 2 and 3. Particular values of the angle  $\phi$ ,  $\phi_{C_{2v,ac}} = 30^\circ, 150^\circ, 270^\circ$  and  $\phi_{C_{2v,ob}} = 90^\circ, 210^\circ, 330^\circ$ , define  $C_{2v}$  configurations. In the former case,  $\phi_{C_{2v,ac}}$ , one of the angles between the three particles, is an acute angle and becomes zero at the equator,  $\theta_{\text{hyp}} = 90^\circ$ , as the positions of two particles coincide. In the latter case,  $\phi_{C_{2v,ob}}$ , one of the angles between the three particles is an obtuse angle and becomes  $180^\circ$  at the equator, meaning that the three particles are in a symmetric linear configuration. The NACTs become very spiky as  $\theta_{\text{hyp}}$  increases, i.e., as the nuclear configurations pass from equilateral to linear. Cuts of the four potential energy surfaces are shown in Fig. 3. Near the pole, the lowest electronic state is well separated from the upper ones. As the equator is approached, the developing singularity due to coinciding nuclear positions at  $\phi = \phi_{C_{2v,ac}}$  can clearly be seen. The NACTs may be classified according

to their symmetry with respect to a reflection at the angles  $\phi = \phi_{C_{2v,ac}}$  and  $\phi = \phi_{C_{2v,ob}}$  as shown in Table II.

To investigate if the three lowest singlet states form a Hilbert subspace, we integrate Eq. (17) for two angles of  $\theta_{\text{hyp}}$ ,  $\theta_{\text{hyp}} = 20^\circ$  and  $\theta_{\text{hyp}} = 60^\circ$ . The Livermore solver DLSODE from ODEPACK [32], appropriate for stiff systems of differential equations, was utilized for this purpose. The order of the transformations in Eq. (16) is in principle irrelevant; however, the numerical integration is more stable if the leading nonadiabatic term, in this case either  $\tau_{12}$  or  $\tau_{23}$ , is rotated first. Our results in Fig. 4 demonstrate that the three lowest states are isolated only at the smaller angle  $\theta_{\text{hyp}} = 20^\circ$ . All transformation angles  $\theta$  become multiples of  $\pi$  after integrating in  $\phi$  over a  $2\pi$  interval. Direct integration over the free  $\tau_{12}$  according to Eq. (15) yields a final value close to zero ( $\theta_{12} = 0.11$ ). If it were zero, it would indicate a two-state quantization. On the other hand, the fact that  $\theta_{12}$  remains close to zero indicates that the coupling is very weak, consistent with Fig. 3. Similarly, if one integrates over the free  $\tau_{23}$ , not shown here, a final value close to  $\pi$  is obtained ( $\theta_{23} = 3.21$ ). These small deviations from zero or  $\pi$ , respectively, are likely not due to numerical inaccuracy, as they are compensated in a three-state quantization. At the angle of  $\theta_{\text{hyp}} = 60^\circ$  neither the two-state nor the three-state quantization condition is satisfied. Our interpretation is that a fourth electronic state plays a role. The question then arises whether the singlet states 2–4 form a Hilbert subspace, or whether we have an effective four-state or more problem. Figure 5 demonstrates that at  $\theta_{\text{hyp}} = 60^\circ$

TABLE II. Symmetry behavior of the NACTs with respect to the angles  $\phi = \phi_{C_{2v,ac}} = 30^\circ + n \times 120^\circ$  and  $\phi = \phi_{C_{2v,ob}} = 90^\circ + n \times 120^\circ$  (s, symmetric; a, antisymmetric).

	$\tau_{12;s}$	$\tau_{13;s}$	$\tau_{23;s}$	$\tau_{14;s}$	$\tau_{24;s}$	$\tau_{34;s}$
	$s = \phi$					
$\phi_{C_{2v,ac}}$	a	s	s	a	a	s
$\phi_{C_{2v,ob}}$	s	a	s	a	s	a
	$s = \rho$					
$\phi_{C_{2v,ac}}$	s	a	s	s	s	a
$\phi_{C_{2v,ob}}$	a	s	a	s	a	s
	$s = \theta_{\text{hyp}}$					
$\phi_{C_{2v,ac}}$	s	a	a	a	s	a
$\phi_{C_{2v,ob}}$	a	s	a	s	a	s



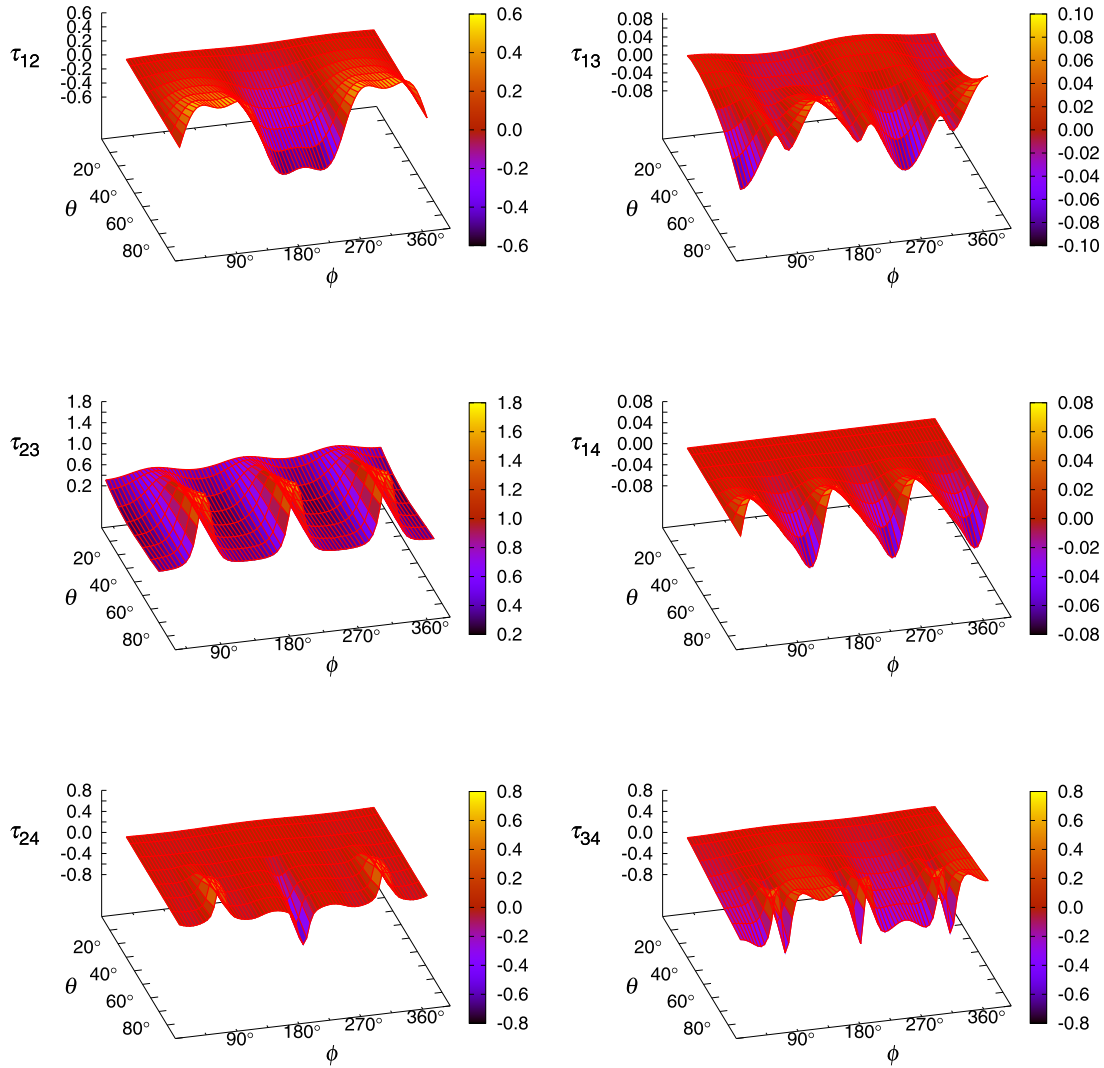


FIG. 2. (Color online) NACTs in the coordinate  $\phi$  between the four lowest singlet states. The value of the hyper-radius,  $\rho$ , was fixed at  $\rho = 3.0a_0$ . The hyperangle  $\theta_{\text{hyp}}$  was varied between  $\theta_{\text{hyp}} = 5^\circ$  and  $\theta_{\text{hyp}} = 70^\circ$ . In hyperspherical coordinates  $\theta_{\text{hyp}} = 0^\circ$  corresponds to the equilateral triangular configuration, while  $\theta_{\text{hyp}} = 90^\circ$  describes linear configurations.

such a three-state description (states 2–4) is appropriate, while at  $\theta_{\text{hyp}} = 20^\circ$  this is not the case. Here, states 1–3 provide a three-state picture. Hence, in the interaction region of

reaction (1), where the three internuclear distances are not too different, up to four electronic states may be needed to describe accurately its dynamics.

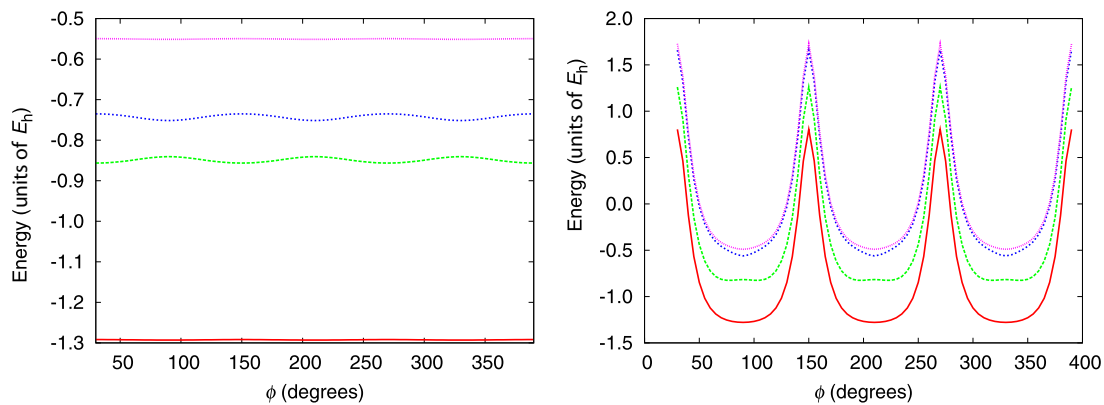


FIG. 3. (Color online) Cuts of the four lowest singlet potential energy surfaces in the coordinate  $\phi$  at  $\rho = 3.0a_0$  and two values of the hyperangle  $\theta_{\text{hyp}}$ ,  $\theta_{\text{hyp}} = 20^\circ$  (left) and  $\theta_{\text{hyp}} = 80^\circ$  (right).

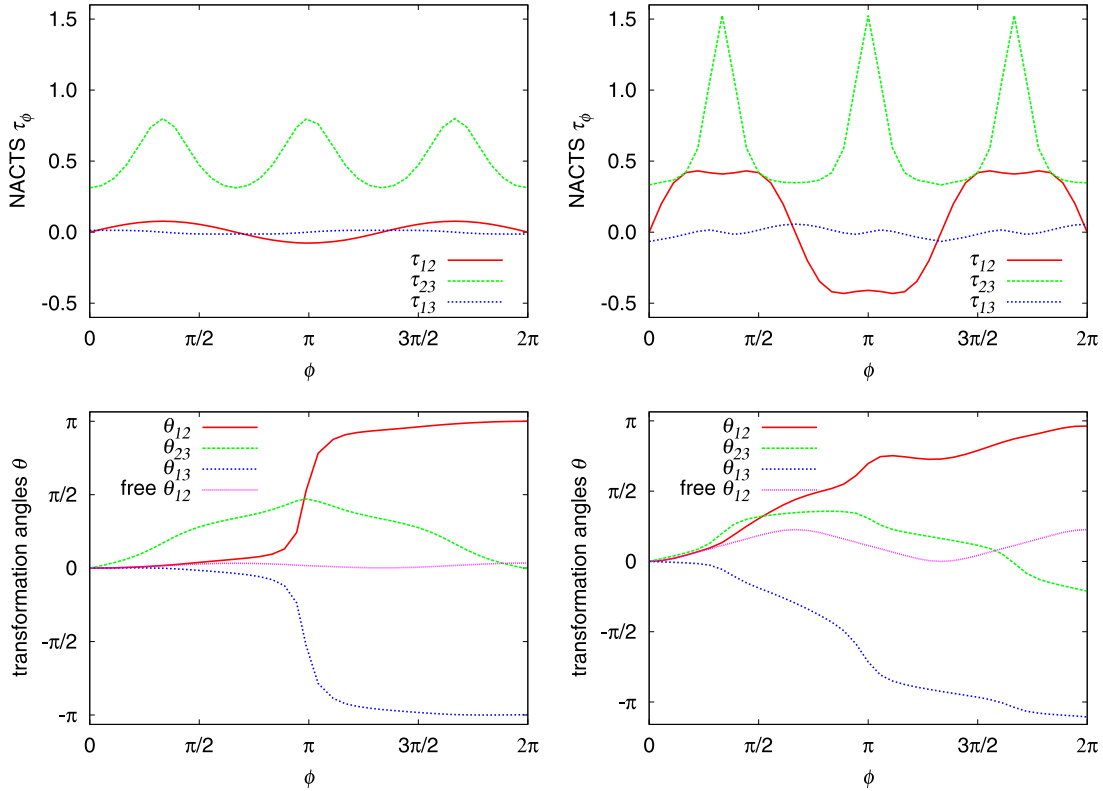


FIG. 4. (Color online) NACTs and transformation angles  $\theta_{ij}$  for the sequence  $(12) \times (23) \times (13)$  and two values of the hyperangle,  $\theta_{\text{hyp}} = 20^\circ$  (left) and  $\theta_{\text{hyp}} = 60^\circ$  (right).

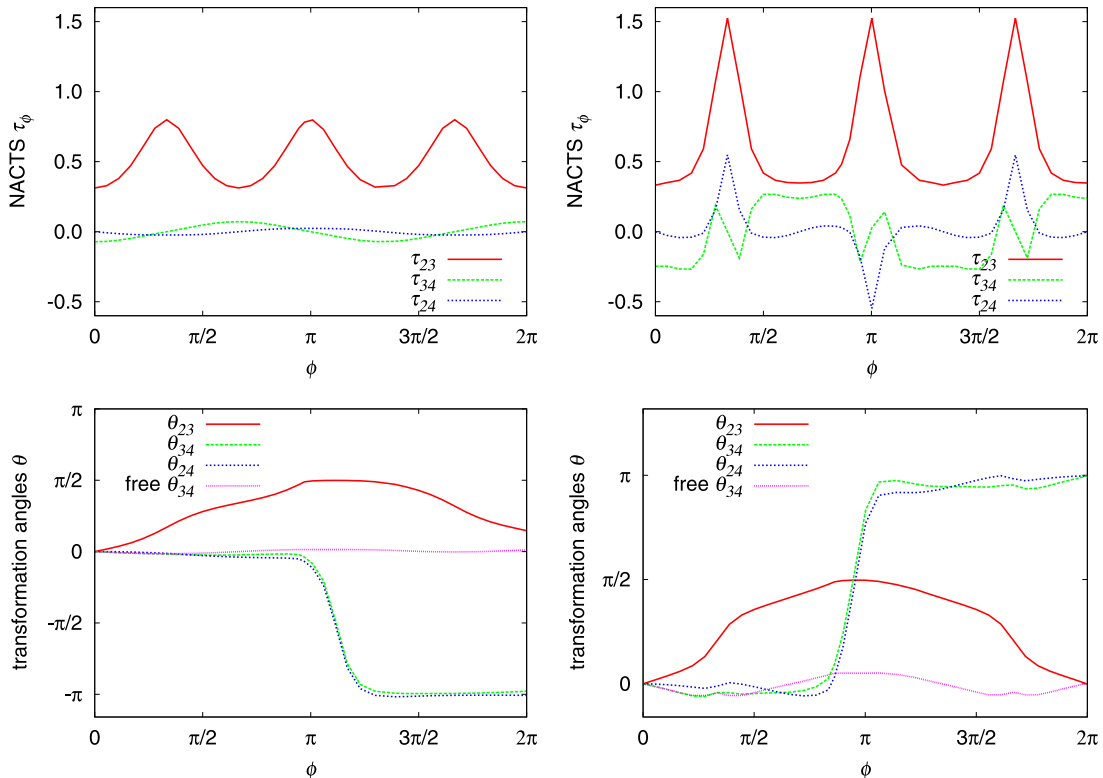


FIG. 5. (Color online) NACTs and transformation angles  $\theta_{ij}$  for the sequence  $(34) \times (23) \times (24)$  and two values of the hyperangle,  $\theta_{\text{hyp}} = 20^\circ$  (left) and  $\theta_{\text{hyp}} = 60^\circ$  (right).

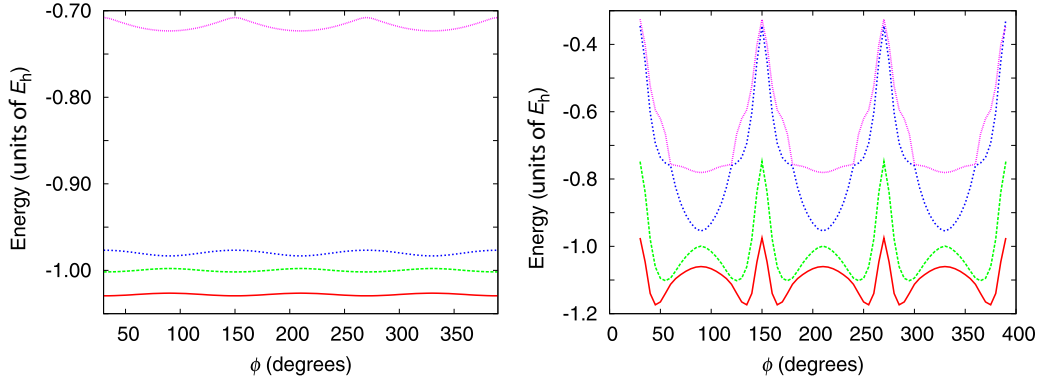


FIG. 6. (Color online) Cuts of the four lowest singlet potential energy surfaces in the coordinate  $\phi$  at  $\rho = 8.0a_0$  and two values of the hyperangle  $\theta_{\text{hyp}}$ ,  $\theta_{\text{hyp}} = 20^\circ$  (left) and  $\theta_{\text{hyp}} = 80^\circ$  (right).

In the asymptotic region of reaction (1), as is well known, nonadiabatic transitions between the two lowest surfaces are favored since these get close in energy; see Eq. (2). The asymptotic region is reached as the hyper-radius,  $\rho$ , is increased. As an example, we show in Fig. 6 cuts through the four lowest electronic state surfaces at  $\rho = 8a_0$ . We turn our attention here to the two lowest states. As we approach the equator,  $\theta_{\text{hyp}} \rightarrow 90^\circ$ , deep gorges are formed, which correspond to the configurations  $\text{H}_2(r = 1.4a_0) + \text{H}^+$  on the lower surface and to  $\text{H}_2^+(r = 2.0a_0) + \text{H}$  on the upper surface. On either surface, the obtuse symmetric configurations ( $\phi_{C_{2v},\text{ob}} = 90^\circ, 210^\circ, 330^\circ$ ) form a kind of rotational barrier between two equivalent structures of the atom-diatom types described above. At the diatomic distance of  $r = 2.5a_0$ , the two surfaces become closest and indeed degenerate as  $\rho \rightarrow \infty$ .

Dynamics in the asymptotic region is best analyzed in Jacobi coordinates. If the collision partners hit at  $C_{2v}$  configuration, which would have to be close to the acute  $\phi$  value  $\phi_{C_{2v},\text{ac}}$ , the nonadiabatic coupling term  $\tau_{12;\phi}$  is small, or indeed zero at  $\phi = \phi_{C_{2v},\text{ac}}$  according to the symmetry properties shown in Table II, and hence nonadiabatic transition is likely due to the action of NACTs in the remaining coordinates,  $\rho$  or  $\theta_{\text{hyp}}$ , which pass there through a maximum. In a near collinear collision, however,  $\tau_{12;\phi}$  is big, which makes a transition between the two states more likely. In Fig. 7, potential energy surface cuts are shown for these two approaches, for both  $r = 2.0a_0$  and  $r = 2.5a_0$ . Figure 8 shows the NACTs between

states 1 and 2 in hyperspherical coordinates. It is interesting to see that the role of  $\tau_{12;\theta_{\text{hyp}}}$  and  $\tau_{12;\phi}$  is interchanged for the two orientational approaches. In the perpendicular approach,  $\tau_{12;\phi}$  is zero by symmetry, while  $\tau_{12;\theta_{\text{hyp}}}$  assumes a maximum (or minimum), according to Table II. In the linear approach, the opposite is true. For the diatomic distance of  $r = 2.0a_0$ , the nonzero term has a maximum (or minimum) at around  $R \approx 6a_0$ , which tends to infinity at  $r = 2.5a_0$ . Equivalent behavior is found for  $\tau_{12;\rho}$ . Orientation does not have a large effect on this coupling term.

## V. CONCLUSIONS

We have analyzed the NACTs in hyperspherical coordinates between the four lowest singlet surfaces of  $\text{H}_3^+$ . In particular we have investigated how many electronic states are necessary to satisfy a quantization criterion for the corresponding NACTs and, hence, need to be included *a priori* to describe the nonadiabatic reactions (1) and (3). As is well known, different mechanisms are possible depending on the energy. At low energy, charge transfer takes place and proceeds via surface hopping between the two lowest electronic potential energy surfaces in the asymptotic region, making it a two-state process. At higher energy, another mechanism, proton exchange, becomes feasible. In the interaction region (transition-state region) of this reaction, nonadiabatic dynamics cannot be restricted, in general, to the two lowest electronic states. As we have verified for certain nuclear configurations, a diabaticization of the lowest

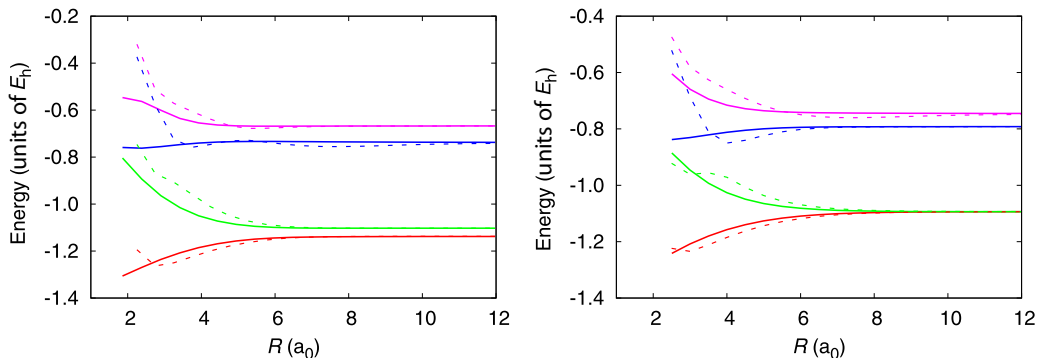


FIG. 7. (Color online) Cuts of the four lowest singlet potential energy surfaces in the atomic-diatom Jacobi coordinate  $R$  for two values of the diatomic distance,  $r$ ,  $r = 2.0a_0$  (left) and  $r = 2.5a_0$  (right), and for two orientations,  $C_{2v}$  (solid lines) and linear (dashed lines).

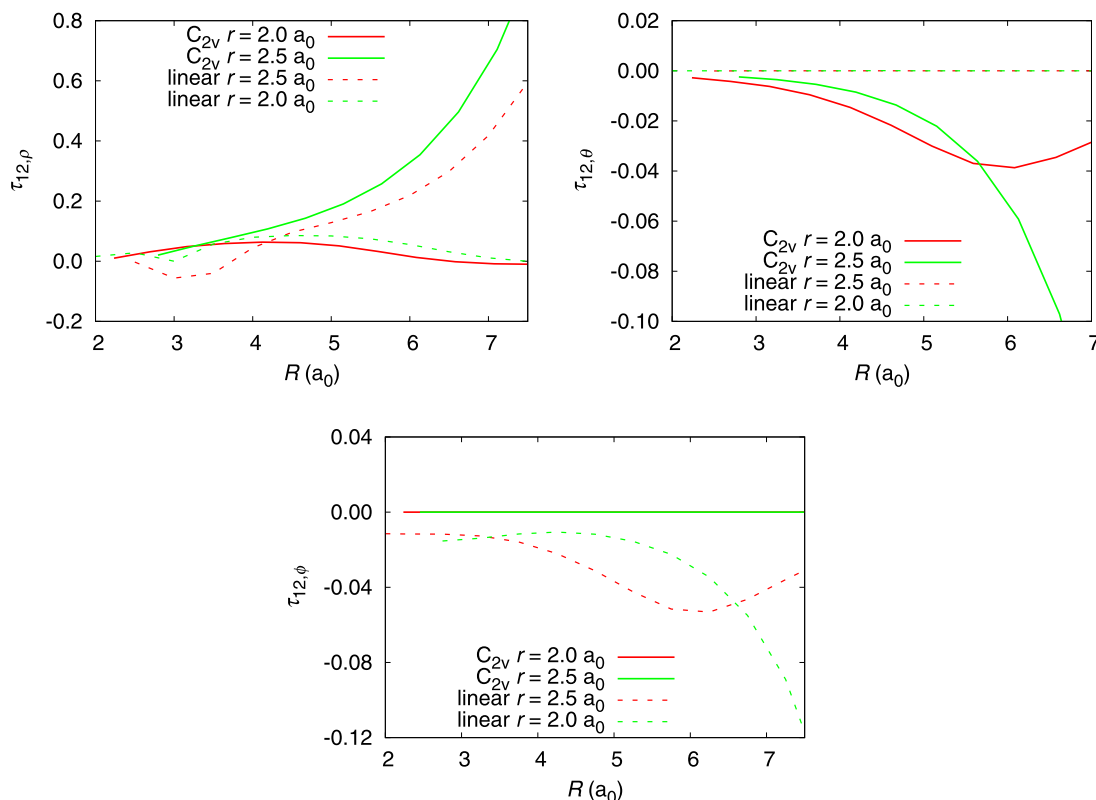


FIG. 8. (Color online) NACTs  $\tau_{12,\rho}$ ,  $\tau_{12;\theta_{\text{hyp}}}$ , and  $\tau_{12,\phi}$  as a function of the Jacobi coordinate  $R$ , for two values of the diatomic distance,  $r = 2.0a_0$  and  $r = 2.5a_0$ , and for two orientations,  $C_{2v}$  and linear.

$\text{H}_3^+$  surfaces requires at least four electronic states, though three-state transformations are sufficient at restricted configuration ranges. To be sure, there are two competing mechanisms for proton exchange of reaction (1): At lower energy, hopping takes place in the entry channel and the system advances to the exit channel without barrier on the lower surface. At higher energy, exchange might take place on the surface of the first excited state by overcoming a large barrier. Hopping to the electronic ground state may then occur in the exit channel. The present results indicate that for such a scenario of competing

mechanisms as many as four electronic states are required for an accurate description, while at lower energy a reduced, two-dimensional treatment is adequate. Work is in progress to generate the complete surfaces of NACTs.

#### ACKNOWLEDGMENT

The authors gratefully acknowledge the provision of supercomputer time by the Computer Center ROMEO of the University of Reims Champagne-Ardenne.

- 
- [1] I. Last, M. Gilibert, and M. Baer, A three-dimensional quantum mechanical study of the  $\text{H} + \text{H}_2^+ \rightarrow \text{H}_2 + \text{H}^+$  system: Competition between chemical exchange and inelastic processes, *J. Chem. Phys.* **107**, 1451 (1997).
- [2] T. Oka, Interstellar  $\text{H}_3^+$ , *Chem. Rev.* **113**, 8738 (2013).
- [3] L. P. Viegas, A. Alijah, and A. J. C. Varandas, Accurate ab initio based multisheeted double many-body expansion potential energy surface for the three lowest electronic singlet states of  $\text{H}_3^+$ , *J. Chem. Phys.* **126**, 074309 (2007).
- [4] M. V. Berry, Quantal phase factors accompanying adiabatic changes, *Proc. R. Soc. A* **392**, 45 (1984).
- [5] M. Baer, G. Niedner-Schatteburg, and J. P. Toennies, A three-dimensional quantum mechanical study of vibrationally resolved charge transfer processes in  $\text{H}^+ + \text{H}_2$  at  $E_{\text{cm}} = 20$  eV, *J. Chem. Phys.* **91**, 4169 (1989).
- [6] G. Niedner, M. Noll, J. P. Toennies, and C. Schlier, Observation of vibrationally resolved charge transfer in  $\text{H}^+ + \text{H}_2$  at  $E_{\text{cm}} = 20$  eV, *J. Chem. Phys.* **87**, 2685 (1987).
- [7] F. O. Ellison, A method of diatomics in molecules. I. general theory and application to  $\text{H}_2\text{O}$ , *J. Am. Chem. Soc.* **85**, 3540 (1963).
- [8] X. Urbain, N. de Ruelle, V. M. Andrianarijaona, M. F. Martin, L. F. Menchero, L. F. Errea, L. Méndez, I. Rabadán, and B. Pons, New light shed on charge transfer in fundamental  $\text{H}^+ + \text{H}_2$  collisions, *Phys. Rev. Lett.* **111**, 203201 (2013).
- [9] T. Gonzalez-Lezana and P. Honvault, The  $\text{H}^+ + \text{H}_2$  reaction, *Int. Rev. Phys. Chem.* **33**, 371 (2014).
- [10] S. Amaran and S. Kumar, Vibrational inelastic and charge transfer processes in  $\text{H}^+ + \text{H}_2$  system: An ab initio study, *J. Chem. Phys.* **127**, 214304 (2007).



- [11] T. González-Lezana, O. Roncero, P. Honvault, J.-M. Launay, N. Bulut, F. Javier Aoiz, and L. Bañares, A detailed quantum mechanical and quasiclassical trajectory study on the dynamics of the  $H^+ + H_2 \rightarrow H_2 + H^+$  exchange reaction, *J. Chem. Phys.* **125**, 094314 (2006).
- [12] P. Barragán, L. F. Errea, A. Macías, L. Méndez, I. Rabadán, A. Riera, J. M. Lucas, and A. Aguilar, Study of *ab initio* molecular data for inelastic and reactive collisions involving the  $H_3^+$  quasimolecule, *J. Chem. Phys.* **121**, 11629 (2004).
- [13] L. F. Errea, C. Illescas, A. Macias, L. Mendez, B. Pons, I. Rabadan, and A. Riera, Influence of nuclear exchange on nonadiabatic electron processes in  $H^+ + H_2$  collisions, *J. Chem. Phys.* **133**, 244307 (2010).
- [14] M. Baer and A. Alijah, Quantized non-adiabatic coupling terms to ensure diabatic potentials, *Chem. Phys. Lett.* **319**, 489 (2000).
- [15] S. Mukherjee, D. Mukhopadhyay, and S. Adhikari, Conical intersections and diabatic potential energy surfaces for the three lowest electronic singlet states of  $H_3^+$ , *J. Chem. Phys.* **141**, 204306 (2014).
- [16] E. E. Nikitin, Nonadiabatic transitions: What we learned from old masters and how much we owe them, *Annu. Rev. Phys. Chem.* **50**, 1 (1999).
- [17] M. Baer, Adiabatic and diabatic representations for atom-molecule collisions: Treatment of the collinear arrangement, *Chem. Phys. Lett.* **35**, 112 (1975).
- [18] C. A. Mead and D. G. Truhlar, Conditions for the definition of a strictly diabatic electronic basis for molecular systems, *J. Chem. Phys.* **77**, 6090 (1982).
- [19] Z. H. Top and M. Baer, Incorporation of electronically nonadiabatic effects into bimolecular reactive systems. I. Theory, *J. Chem. Phys.* **66**, 1363 (1977).
- [20] M. Baer, S. H. Lin, A. Alijah, S. Adhikari, and G. D. Billing, Extended approximated Born-Oppenheimer equation. I. Theory, *Phys. Rev. A* **62**, 032506 (2000).
- [21] S. Adhikari, G. D. Billing, A. Alijah, S. H. Lin, and M. Baer, Extended approximated Born-Oppenheimer equation. II. Application, *Phys. Rev. A* **62**, 032507 (2000).
- [22] M. Baer, *Beyond Born-Oppenheimer: Electronic Nonadiabatic Coupling Terms and Conical Intersections* (John Wiley & Sons, New York, 2006).
- [23] M. Berblinger, E. Pollak, and C. Schlier, Bound states embedded in the continuum of  $H_3^+$ , *J. Chem. Phys.* **88**, 5643 (1988).
- [24] M. Pavanello, L. Adamowicz, A. Alijah, N. F. Zobov, I. I. Mizus, O. L. Polyansky, J. Tennyson, T. Szidarovszky, and A. G. Császár, Calibration-quality adiabatic potential energy surfaces for  $H_3^+$  and its isotopologues, *J. Chem. Phys.* **136**, 184303 (2012).
- [25] M. Pavanello and L. Adamowicz, High-accuracy calculations of the ground,  $1^1A'_1$ , and the  $2^1A'_1$ ,  $2^3A'_1$  and  $1^1E'$  excited states of  $H_3^+$ , *J. Chem. Phys.* **130**, 034104 (2009).
- [26] L. G. Diniz, J. R. Mohallem, A. Alijah, M. Pavanello, L. Adamowicz, O. L. Polyansky, and J. Tennyson, Rotational and vibrational non-adiabatic calculations on  $H_3^+$  using coordinate-dependent vibrational and rotational masses, *Phys. Rev. A* **88**, 032506 (2013).
- [27] L. Lodi, O. L. Polyansky, J. Tennyson, A. Alijah, and N. F. Zobov, QED correction for  $H_3^+$ , *Phys. Rev. A* **89**, 032505 (2014).
- [28] R. Jaquet and T. Carrington, Using a nondirect product basis to compute  $J > 0$  rovibrational states of  $H_3^+$ , *J. Phys. Chem. A* **117**, 9493 (2013).
- [29] B. R. Johnson, New numerical methods applied to solving the one-dimensional eigenvalue problem, *J. Chem. Phys.* **67**, 4086 (1977).
- [30] F. T. Smith, Generalized angular momentum in many-body collisions, *Phys. Rev.* **120**, 1058 (1960).
- [31] H.-J. Werner, P. J. Knowles, G. Knizia, F. R. Manby, M. Schütz *et al.*, “MOLPRO, version 2012.1, a package of *ab initio* programs” (2012), <http://www.molpro.net>.
- [32] A. Hindmarsh, Odepack, a systematized collection of ode solvers, in *Scientific Computing: Applications of Mathematics and Computing to the Physical Sciences*, IMACS Transactions on Scientific Computing Vol. 1, edited by R. S. Stepleman *et al.* (North-Holland, Amsterdam, 1983), pp. 55–64.